Available online at www.sciencedirect.com
ScienceDirect
Journal of Molecular Catalysis A: Chemical 264 (2007) 128–134
JOURNAL OF MOLECULAR CATALYSIS A: CHEMICAL
www.elsevier.com/locate/molcata

Aqueous H_2O_2 as an oxidant for CO over Pt– and Au–NaY catalysts

Tarek M. Salama, Zeinhom M. El-Bahy, Farouk I. Zidan *

Chemistry Department, Faculty of Science, Al-Azhar University, Nasr City 11884, Cairo, Egypt

Received 27 May 2005; accepted 2 August 2006
Available online 13 October 2006

Abstract

The oxidation of carbon monoxide with aqueous hydrogen peroxide was carried out over Pt– and Au–NaY catalysts, that were prepared by the impregnation of NaY zeolite (Si/Al = 5.6, S_{BET} = 910 m^2/g) with aqueous solutions of tetramine platinum(II) nitrate and hydrogen tetrachloroaurate trihydrate, respectively. The Pt– and Au–NaY catalysts exhibited high activity at relatively low temperatures as low as 303 K in the CO–H_2O_2 reaction. Pt–NaY was compared favorably with Au–NaY at similar reaction conditions, where the specific reaction rate constant, K_m, over Pt–NaY was five times of magnitude higher than that of Au–NaY at 323 K. These data were confirmed by the values of activation energy evaluated from Arrhenius plots. The Pt–NaY was reduced in flowing H_2 at 623 K for 2 h. The catalytic activity of reduced Pt–NaY was about 44 times more active than that of analogous unreduced catalyst at 303 K. The catalytic activity of Au–NaY was greatly affected by thermal treatment. A higher K_m value was obtained at 353 K over Au–NaY, exceeding this temperature led to a decrease in activity due to sintering of Au particles. It is proposed that a dual Au(0)/Au(I) site is necessary to catalyze the reaction, where, Au(0) accelerates the H_2O_2 decomposition and the CO adsorption capability was enhanced on Au(I) site.

Keywords: CO oxidation; Gold; Platinum; NaY; Hydrogen peroxide

1. Introduction

Oxidation processes play a significant role in chemical industry, being the basis for production of important compounds [1]. Benefits deriving from availability, low cost and absence of wastes select molecular oxygen as the oxidant of choice. However, the sever reaction conditions often required or the radical nature of the reaction involved, are common obstacles to a wide use of the molecular oxygen in synthetic chemistry. As an alternative, monooxygen donors are available as milder oxidants: hydrogen peroxide, peracids, organic hydroperoxides, inorganic and metallorganic peroxides, sodium hypochlorite and nitrous oxide. In catalytic oxidation, these are generally characterized by good activity at moderate temperatures and, often by good selectivity as well. Among many oxidants, hydrogen peroxide (H_2O_2) is a quite unique. It has high active oxygen content (47%) and producing water as the only by-product [2].

Carbon monoxide is usually one of the discarded by-products in bulk chemical processes as an environmental issue [3]. The catalytic oxidation of carbon monoxide on transition metal surfaces has gained increasing importance in recent years in chemical industry and automobile emission control as well as a model reaction for surface science investigations. The reaction takes place between dissociatively adsorbed oxygen and molecularly adsorbed carbon monoxide by which CO_2 immediately desorbs after formation.

Moreover, the hydrogen used as a fuel in polymer electrolyte membrane fuel cell (PEMFC), as used in electric vehicles, operates at relatively low temperatures between 328 and 378 K [4]. Hydrogen rich fuel produced from methanol, by the steam reforming and water gas shift reaction processes, should be essentially free of CO to avoid poisoning of the Pt anode at these low temperatures. CO, if present, strongly adsorbs onto anode Pt catalyst surface in the fuel cell and substantially reduces the overall fuel cell performance [5]. Under normal running conditions the product hydrogen stream contains 25 vol.% CO_2, a few vol.% H_2O, and about 0.5–1 vol.% CO. Thus, in order to obtain optimum performance, the total concentration of CO in the gas stream should be reduced if possible to below 100 ppm.

The main target of the present work is to explore whether H_2O_2 could serve as a potential oxygen donor for the oxidation of CO in solution by comparing the catalytic properties of

* Corresponding author. Tel.: +202 2629357/8; fax: +202 2629356.
E-mail address: zeinelbahy2020@yahoo.com (Z.M. El-Bahy).

1381-1169/$ – see front matter © 2006 Elsevier B.V. All rights reserved.
doi:10.1016/j.molcata.2006.08.003

Au–NaY with Pt–NaY. However, supported gold catalysts are, in contrast to Pt-group metal catalysts, intrinsically more active for CO oxidation than for H_2 oxidation [6], and the catalytic activity of Au is enhanced by moisture [7,8] and almost insensitive to CO_2 [9]. Furthermore, it has been emphasized that the conversion of CO oxidation was dramatically increased by an order of six times of magnitude with the introduction of water vapor compared with the system free of steam [10]. Although the catalytic oxidation of carbon monoxide by molecular oxygen gas has been extensively studied in the last decades [11–14], to the best of our knowledge the oxidation of CO with aqueous H_2O_2 has not yet been reported in literature.

2. Experimental

2.1. Materials and regents

Tetraamine platinum(II) nitrate $[Pt(NH_3)_4](NO_3)_2$ from strem Chemical, USA. Gold(III) was in the form of hydrogen tetrachloroaurate trihydrate ($HAuCl_4{\cdot}3H_2O$) from Aldrich, A.C.S. Hydrogen peroxide was provided as an aqueous solution (30%, w/w) BDH grade. NaY zeolite (Si/Al = 5.6), surface area = 910 m^2/g, HZS-320 NAA, lot no. 3001, Japan.

2.2. Preparation of catalysts

5 and 10 wt.% Pt and 10 wt.% Au were deposited by incipient wetness impregnation onto NaY zeolite with solutions of $[Pt(NH_3)_4](NO_3)_2$ and $HAuCl_4{\cdot}3H_2O$, respectively. The Pt and Au supported on NaY precursors slurry were refluxed at 333–353 K with continuous stirring for 3 h. The preparations were thoroughly washed with hot water and therefore Au sample is considered to be almost free of chloride ions. The prepared Pt and Au supported precursors were air-dried overnight at 383 K unless otherwise stated and heated in air at 333–673 K for 3 h. The prepared samples were referred to as M*x*–NaY(*t*), where M, *x* and *t* stand for the name of the precious metal, its weight percentage and the treatment temperature, respectively. The Pt–NaY sample was reduced in a closed glass manifold circulation system by introducing hydrogen (99.99% purity, 120 Torr) while installing liquid nitrogen trap to prevent evolved water from re-oxidation of the samples.

2.3. Catalyst characterization

2.3.1. X-ray diffraction

X-ray diffractograms were obtained using a Philips Analytical (type PW 1840) diffractometer. The patterns were run with nickel-filtered Copper radiation (λ = 1.5405 Å) at 30 kV and 20 mA with scanning speed of 2° in 2θ min^{-1}. Calculations for average crystallite size were made using Pt(1 1 1) linewidths in Scherrer equation [15], with Gaussian lineshape approximation.

2.3.2. Thermal analysis

Thermogravimetric analyses were performed with a Shimadzu-50 thermal analyze. TG and DTG curves were recorded with the following conditions: 9 mg; nitrogen atmosphere of flow rate 30 ml min^{-1}; platinum crucible; ramp rate 10° min^{-1} and a maximum temperature of 1073 K.

2.4. Catalytic reactions

The oxidation of CO with aqueous H_2O_2 was carried out in a continuous flow mode system. In a typical reaction, 100 ml of 0.5 M H_2O_2 aqueous solution was introduced into a double jacket glass reactor. The pH of the solution was ≈6.2. Using gas flowmeters, the gas mixture consisting of CO and N_2 (CO/N_2 = 0.1) was allowed to pass through the catalyst bed with space velocity (SV) of 12 000 ml g^{-1} h^{-1}. The temperature of the glass reactor was adjusted at the desired temperature by using a temperature controller type (PEX-P 90). 0.1 g of catalyst stock (unless otherwise stated) was added to the reaction medium supposing zero time. To pursue the progress of the reaction with time, the resulting gas mixture was introduced in a strong alkaline solution with an online pH meter. Since the decrease of OH^- (indicated by the decrease of pH value) is equivalent to the amount of CO_2 evolved from the reaction. The natural logarithm of $[OH^-]$ (ln *C*) was plotted against (time, min) as an application of the first order rate equation ($K_t = \ln C_0 - \ln C$). The specific rate constant K_m was calculated as (K_m = rate consant (*K*)/catalyst weight) and used to express the activity of the prepared catalysts.

3. Results and discussion

3.1. X-ray diffraction

In Fig. 1, the x-ray diffraction patterns of Pt10–NaY(673) and NaY are compared. The Pt free sample displayed the expected pattern of NaY zeolite [16]. The crystallographic changes induced by Pt10–NaY(673) exhibited virtually the unshifted Pt lines in the normal face-centered cubic (fcc) pattern of metallic Pt at 2θ = 39.8° (1 1 1) and 46.4° (2 0 0) [15]. The

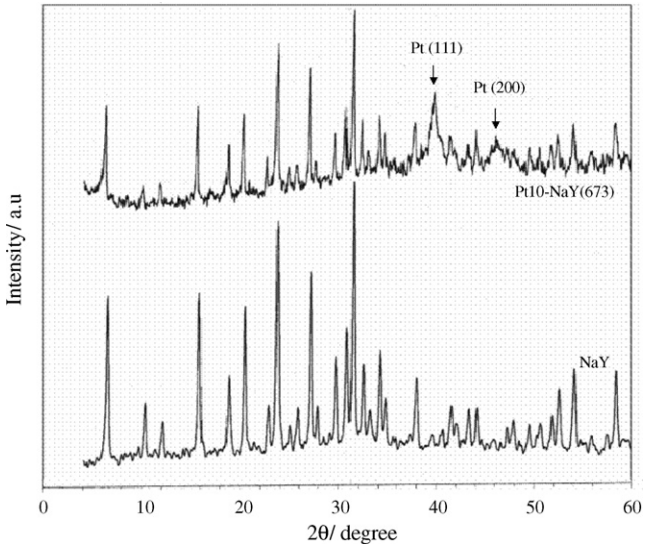

Fig. 1. XRD spectra of NaY and Pt10–NaY catalyst heated at 673 K.

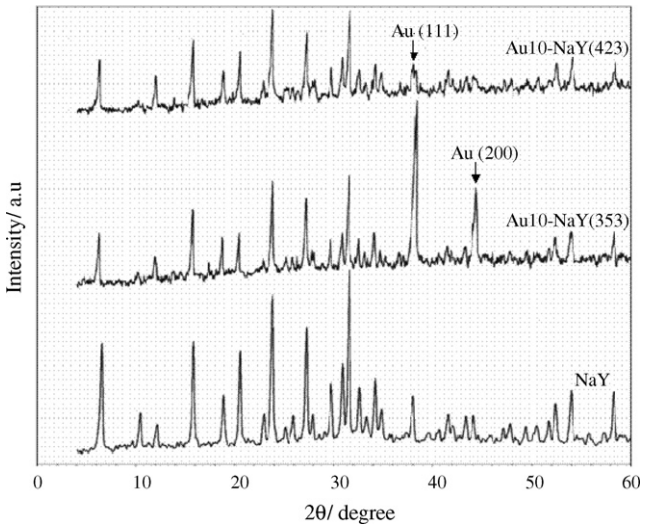

Fig. 2. XRD spectra of NaY and Au(10)–NaY catalyst treated at 353 and 423 K.

formation of Pt crystallites was likely occurred due to decomposition of Pt precursor complex, $[Pt(NH_3)_4](NO_3)_2$, during the calcination at 673 K. The unshifted position of all Pt peaks indicated that Pt forms a separate phase at the external surface of NaY zeolite. Average Pt crystallite size was calculated from the Pt10–NaY(673) pattern using line broadening of the Pt(1 1 1) line, Scherrer equation, and a correction for instrumental line broadening. The 18.6 nm average size of Pt crystallites thus calculated was much smaller than those reported for $Pt(1.2–5.0)/WO_3/SiO_2$ catalysts, e.g. 50 nm, which decreased with WO_3 loading [17]. This indicates that, the distribution of Pt particles in NaY zeolite is better than that on the SiO_2 substrate. Nevertheless, other oxidized forms of Pt moieties could also present in NaY, though we did not reduce this sample. A careful inspection of the pattern did not demonstrate evidence of either PtO or PtO_2, which may not show appreciable crystallinity at this calcination stage. Thus, we cannot exclude completely the presence of these phases since powder diffraction X-ray technique will not detect amorphous solids and those having particle size less than 50 Å.

Fig. 2 shows the XRD diffractograms of pure NaY and Au10–NaY(353) and Au10–NaY(423). The XRD pattern of Au10–NaY(353) was characterized by the presence of new diffraction lines at $2\theta = 38.2°$ (1 1 1) and 44.4° (2 0 0) due to metallic Au particles [6]. The average crystallites size of Au were estimated (using Scherrer equation) to be 55.7 and 46.4 nm from the peak-width of Au(1 1 1) for the sample heated at 353 and 423 K, respectively. As far as the impregnation method was used it was difficult to deposit Au on zeolite with dispersion as high as that for Pt metal, though gold has low sublimation energy and very low Tammann temperature [18]. It was evidenced in a previous study by EXAFS/XANES technique that the Au particles existed in the supercage of NaY when $AuCl_3$/NaY was thermally treated at 328–353 K [16]. The decrease of Au particle size with temperature shows, as unexpected, that Au particles diffuse inside or nearby the surface (α-cages) with increasing the temperature.

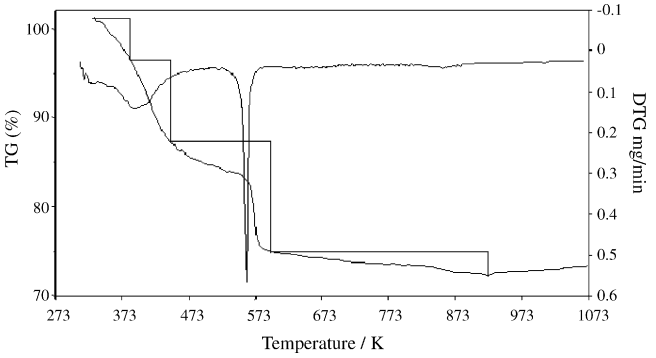

Fig. 3. The TG and DTG profiles of Pt10–NaY.

3.2. Thermal behavior of uncalcined samples

Figs. 3 and 4 show the representative TG and DTG curves of the Pt10– and Au10–NaY solid samples along with the weight percentage loss at different steps. The DTG profiles exhibited four endothermic peaks of maximal located at 330, 391, 554 and 695 K for Pt10–NaY (Fig. 3), whilst at 348, 393, 469 and 699 K for the Au10–NaY (Fig. 4). The first, second and fourth peaks in the profiles of both samples are found at nearly identical temperatures. The first and second maximal correspond to elimination of loosely bound and strongly held water molecules in NaY zeolite, respectively, where they resemble those in the curve of unloaded NaY (not shown).

The third maximum of weight loss in the curve of Pt10–NaY at 554 K corresponds to the maximum rate of decomposition of $[Pt(NH_3)_4]^{2+}$ complex to metallic Pt (Fig. 3). The formation of Pt(0) particles in the calcined sample at 673 K has been confirmed by the XRD analysis, $2\theta = 39.8°$ and 46.4°. However, the formation of some metallic Au in the early stage shortly after heating of Au10–NaY is likely occurred since the decomposition of some Au precursors exposed to the surface of zeolite was reportedly taking place at low temperatures as 338–353 K [19]. This conclusion has been confirmed by the XRD analysis of this sample. Where a diffraction line was observable at $2\theta = 38.2°$ and 44.4° characteristic to Au(0). The loss of intrazeolite chloride associated with Au sample in the β-cage represents the third temperature region of weight loss in the profile of Au10–NaY. In fact, the investigated samples exhibited a slow loss process

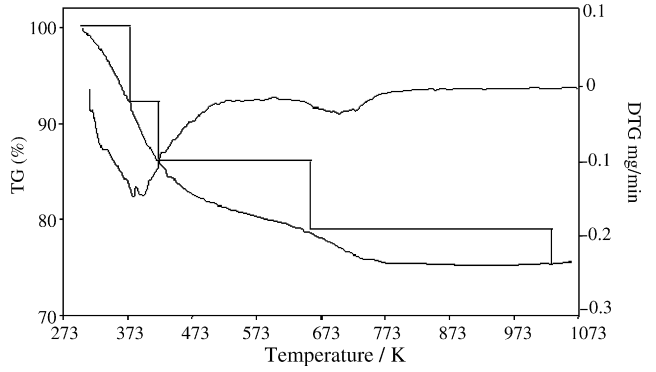

Fig. 4. The TG and DTG profiles of Au10–NaY.

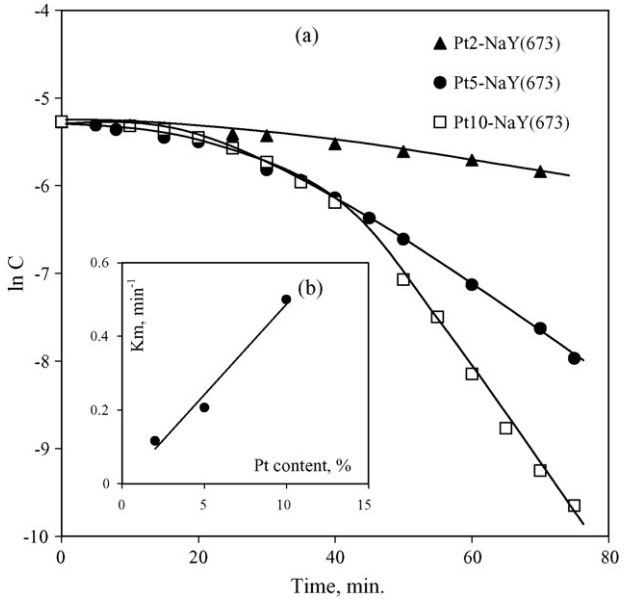

Fig. 5. (a) First order plots of CO oxidation with (0.5 M) H_2O_2 at 313 K over Pt–NaY of different Pt loadings and (b) the correlation between the K_m values and the Pt loadings.

by heating in a wide range (573–973 K) followed by mass loss of 2.1 and 3.8 wt.% for Pt and Au samples, respectively. This process might indicate complete removal of OH groups from NaY lattice.

3.3. Oxidation of CO over Pt-NaY catalysts

3.3.1. Influence of Pt content

Fig. 5a shows the first order plots (ln C versus time) of CO oxidation with H_2O_2 at 333 K over the Pt2–, Pt5– and Pt10–NaY(673) catalysts. It is worthy to mention that, water gas shift reaction did not contribute in the production of CO_2 in the studied temperature. It is obvious that first order kinetics is obeyed only after a certain period of about 20–40 min. During such period the rate of CO oxidation is less than H_2O_2 decomposition, therefore O_{ad} resulting from the decomposition of H_2O_2 is favorably adsorbed more than CO on the catalyst surface leading to slow rate of CO oxidation at the first stage of reaction. After that period the reaction assumes a significant rate and obeys first order kinetics. Similar results were observed in case of Au–NaY and also over Cu–NaY catalysts [20] for the same reaction. The specific first order rate constant K_m was evaluated from the linear portion of the curves.

The correlation of the catalytic activity (K_m value) with Pt content is shown in Fig. 5b. It is clear that the catalytic activity of Pt–NaY catalysts increases systematically as the Pt content increases. This might suggest that the Pt particles have well dispersed in Y-zeolite, which gave good activity in the CO oxidation reaction with aqueous H_2O_2.

3.3.2. Influence of reaction temperature

From the kinetic study of CO oxidation over Pt–NaY catalysts, it was concluded that the catalytic activity of these catalysts

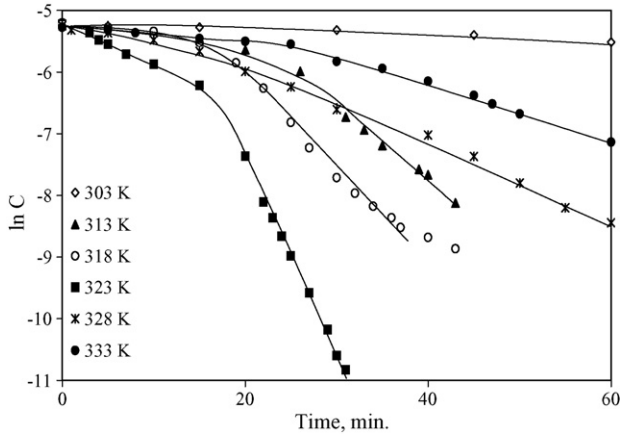

Fig. 6. First order plots of CO oxidation with aqueous (0.5 M) H_2O_2 over unreduced Pt10–NaY catalyst at different reaction temperatures.

increases with increasing the Pt-content. It is also noticed that the XRD pattern of these catalysts showed the characteristic lines of Pt metal (ca. $2\theta = 39.8^\circ$ and 46.4°). Therefore it seems interesting to explore the effect of reduction of Pt10–NaY catalyst on its catalytic activity towards CO oxidatin with aqueous H_2O_2 at different temperatures. One hundred and 20 mg of unreduced and reduced catalysts, respectively, were used for the CO oxidation reaction at relatively low temperatures in the range of 303–333 K. Taking in consideration that a small amount of reduced catalyst (20 mg) was used due to its high activity towards the H_2O_2 decomposition which in turn difficult to follow up the reaction. Figs. 6 and 7 illustrate the first order plots (ln C versus time) of CO oxidation with aqueous H_2O_2 (0.5 M) over unreduced and reduced catalysts, respectively, and at the studied temperatures. The K_m values as a function of temperature were calculated and represented in Table 1. A similar trend of activity, increasing then decreasing with temperature, is obvious. Two temperature regions were observed in case of both catalysts with a maximum value of K_m at 313 K for the reduced catalyst while it was at 323 K for the unreduced one. The K_m values listed in Table 1 demonstrate that, a dramatic increase of the catalytic

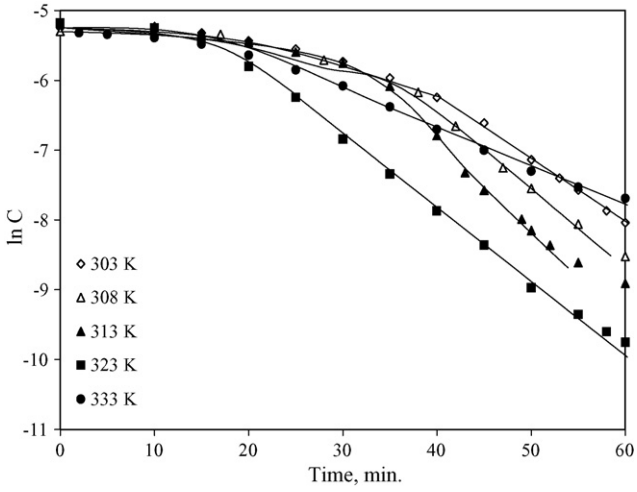

Fig. 7. First order plots of CO oxidation with aqueous (0.5 M) H_2O_2 over reduced Pt10–NaY catalyst at different reaction temperatures.

Table 1
Reaction rate constants of CO oxidation using (0.5 M) H_2O_2 on the surface of reduced and unreduced Pt10–NaY catalysts at different reaction temperatures

	Temperature (K)						
	303	308	313	318	323	328	333
K_m (min^{-1})							
Unreduced Pt/NaY	0.09	–	0.98	1.54	3.01	0.65	0.44
Reduced Pt/NaY	4.01	5.1	6.6	–	4.9	–	2.7

activity of the reduced catalyst compared with the unreduced one was observed especially at low temperature (303 K). For instance, at that temperature, the value of the specific rate constant (K_m) was 4.45 min^{-1} for reduced Pt10–NaY while it was weighing up 0.09 min^{-1} at the same temperature over unreduced Pt10–NaY. Based on the above experimental observations, it is evident that Pt metal in NaY functions as the active site for CO oxidation with aqueous H_2O_2 as a large area of Pt surface becomes accessible for CO adsorption. However, the XRD data have shown that the particle size of Pt metal was obtained as small as 18.6 nm. Also, the linear relationship between Pt content and the activity of such catalysts gives further evidence that the active sites are Pt species which are dispersed on the catalyst surface.

The Arrhenius plots for reduced and unreduced catalysts, Fig. 8, illustrated a reverse trend at the high temperature region (303–323 K). Similar results were invoked by several authors for gaseous CO oxidation with O_2 over Pt–Al_2O_3 catalysts [21,22]. The calculated activation energies were ≈20 and ≈55 kJ mol^{-1} for reduced and unreduced catalysts, respectively. From these results, it is obvious that the reaction mechanism changed completely with temperature. The inversion of the Arrhenius trend at relatively high temperatures is discussed on the basis of the higher decomposition of H_2O_2 on Pt surface, resulting in the coverage of Pt with O_{ad}. The subsequent assess of CO to Pt sites appreciably decreased, indicating a competitive O–CO adsorption on Pt surface. In addition, the rate of H_2O_2 decomposition increased with temperature in which the nature of the active sites is mutually changed to an oxidic form, $Pt(O)_x$ [10], leading to a drastic monotonic decrease in the reaction rate. From the data, it is clear that the CO oxidation in aqueous H_2O_2 solution reduces the activation energy for the reaction drastically especially in case of the reduced catalyst. However, similar results were reported where the activation energy of CO oxidation was estimated to be ≈74 and 37 kJ mol^{-1} in the absence and presence of water vapor, respectively [10].

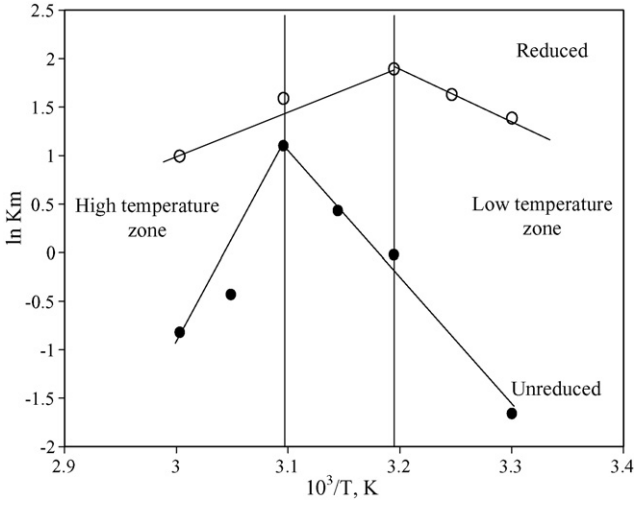

Fig. 8. Arrhenius plots of CO oxidation over reduced and unreduced Pt10–NaY catalysts.

It is of great interest to note that the activation energy of CO oxidation in aqueous H_2O_2 solution has low E_{ac} value for reduced catalyst compared with that of the non-reduced one gave further evidence that highly dispersed metallic Pt is served as the active site for this reaction.

3.4. Oxidation of CO over Au–NaY catalysts

Gold is well known for its inertness among group Ib metals [18], so, the Au atoms may be considered as less active than other precious metals for adsorption and catalysis. Recently, Haruta et al. [23,24] have found that gold is very active for the low temperature oxidation of CO, if dispersed on metal oxides such as TiO_2. Therefore, it seems interesting to test the activity of Au supported on NaY zeolite towards the oxidation of CO with H_2O_2 in aqueous media.

The effect of thermal treatment of Au10–NaY catalyst on CO oxidation was studied by heating the samples in air for 3 h

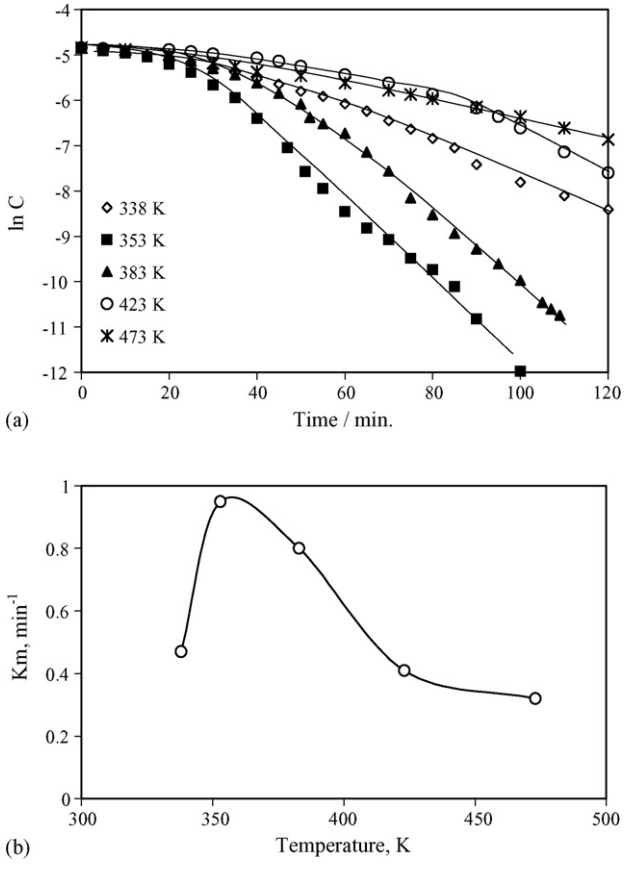

Fig. 9. (a) First order plots of CO oxidation with aqueous H_2O_2 (0.5 M) over Au10–NaY treated at different temperatures and (b) relationship between the K_m values and the treatment temperatures.

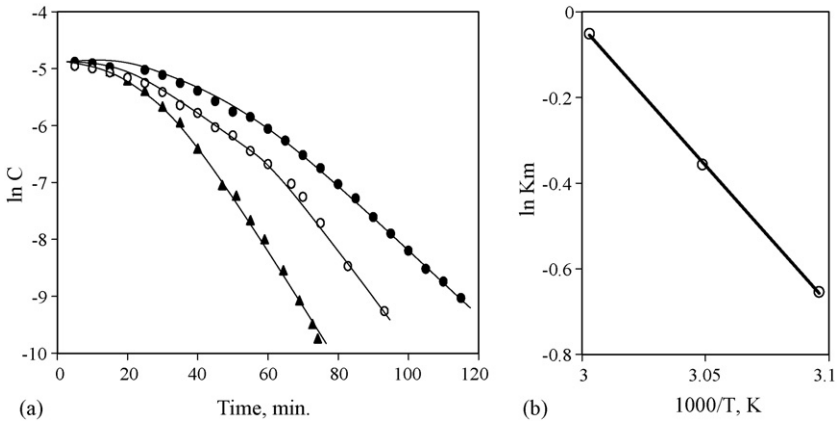

Fig. 10. (a) First order plots of CO oxidation with aqueous H_2O_2 over Au10–NaY at different temperatures and (b) Arrhenius plot of CO oxidation over Au10–NaY catalyst.

at temperatures ranging between 338 and 503 K. Fig. 9a illustrates the first order plots of CO oxidation at 333 K with 0.5 M H_2O_2 in presence of Au10–NaY catalysts treated at different temperatures. 0.1 g of the prepared samples was used. The K_m values were 0.47, 0.95, 0.8, 0.41, 0.32 and 0.20 min^{-1} at 338, 353, 383, 423, 473 and 503 K, respectively. It is clear that the activity of Au10–NaY catalyst heated at 353 K was found to have superior activity over other Au treated catalysts at higher temperatures (Fig. 9b).

The high activity of Au10-NaY catalyst heated at 353 K should be attributed to the reduction of Au(III) to Au(I) and Au(0) in the presence of H_2O [14,16]. Au(I) is considered as the active site for CO adsorption over Au–NaY catalysts as confirmed in our previous work [25]. It was shown by XRD analysis that the sample heated at 353 K possesses gold crystallites and since, this sample showed the highest catalytic performance among all the Au–NaY catalysts. It is suggested that, a dual site Au(I)–Au(0) is crucial for this reaction. The present results indicate that three steps are possible for CO oxidation by aqueous H_2O_2 over gold catalysts: (i) the oxidation of Au(0) by O_{ad} derived from H_2O_2 leading to the formation of Au–O–Au linkages [8]; (ii) the hydrolysis of Au–O–Au to Au(I)–OH^-; (iii) CO replaces the OH^- forming Au(I)–CO which reacts with O_{ad} forming CO_2. The elimination of Au(I)–OH^- is expected due to a very low activation energy of Au–O bonds [16,26] (Scheme 1). According to the proposed mechanism, one must consider that the delay of the desorption of CO_2 (t_{ind}) is due to sequential formation of Au(I).

The influence of reaction temperature on the activity of Au10–NaY(353) catalyst was studied at three different temperatures namely 323, 328 and 333 K at similar reaction conditions (Fig. 10a). The activities, K_m, values were 0.52, 0.70, 0.95 min^{-1} at 323, 328 and 333 K, respectively. The K_m values increase with increasing the reaction temperature. The activation energy of CO oxidation calculated from the Arrhenius plot was 27 kJ mol^{-1}. The value of activation energy obtained in this study is less that the values observed by Iwasawa and co-workers (50–87 kJ mol^{-1}) [27,28] which indicates that the aqueous CO oxidation by H_2O_2 is much easier than other methods since it has lower activation energy. The activation energy of the CO

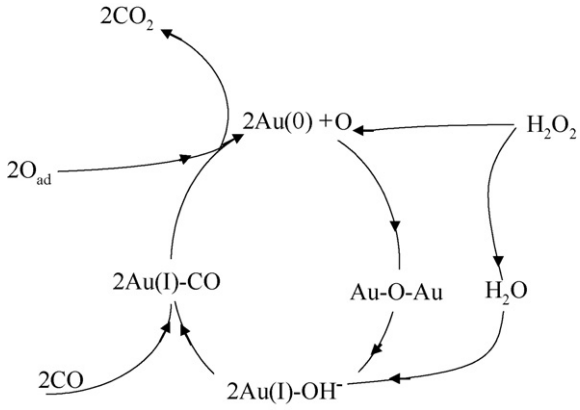

Scheme 1. Proposed scheme for CO oxidation with (0.5 M) H_2O_2 over Au–NaY catalyst.

oxidation reaction over Au10–NaY catalyst is higher than that over reduced Pt10–NaY catalyst indicating that the oxidation of CO with aqueous H_2O_2 proceeds more readily over the reduced Pt catalyst than over Au–NaY.

4. Conclusions

The results in this study present the CO oxidation in aqueous H_2O_2 solution over precious metals namely Au and Pt catalysts supported on NaY zeolite. The reaction proceeded successfully at ambient temperature on the prepared catalysts. Pt–NaY catalyst showed much better catalytic activity than Au–NaY catalyst in the CO oxidation under the studied conditions. Four possible reasons may be considered as good evidences for suggesting that dispersed metallic Pt is served as the active site for CO oxidation:

(i) The catalytic activity of Pt–NaY catalysts increases as the Pt content increases.
(ii) The XRD study of Pt10–NaY catalyst confirms the presence of Pt-metal on the surface of NaY zeolite.
(iii) The catalytic activity of the reduced Pt10–NaY in the oxidation of CO is approximately 44 times that of the unreduced catalyst at 303 K, and under the same conditions.

(iv) Activation energy of CO oxidation over the reduced catalyst (ca. 20 kJ mol^{-1}) is much lower than that over the unreduced catalyst (ca. 55 kJ mol^{-1}).

The heat treatment of Au–NaY catalyst showed that the highest catalytic activity was obtained for the catalyst treated at 353 K. A dual Au(I)/Au(0) site was suggested as the active center for CO oxidation over Au–NaY catalysts.

References

[1] G. Perego, G. Bellussi, C. Corno, M. Tamarasso, F. Buonomo, A. Esposito, Stud. Surf. Sci. Catal. 28 (1986) 129.
[2] M.G. Clerici, P. Ingallina, Catal. Today 351 (1998) 41.
[3] D. Bianchi, R. Bortolo, R. D'Aloisio, M. Ricci, J. Mol. Catal. A 150 (1998) 87.
[4] S. Gottesfeld, J. Pafford, J. Electrochem. Soc. 135 (1988) 2651.
[5] G.J.K. Acres, J.C. Forst, G.A. Hards, R.J. Potter, T.R. Ralph, D. Thompsett, G.T. Burstein, G.J. Hutching, Catal. Today 38 (1997) 393.
[6] M. Haruta, N. Yamada, T. Kobayashi, S. Iijima, J. Catal. 115 (1989) 301.
[7] M. Haruta, T. Takase, T. Kobayashi, Catalytic Science and Technology, vol. 1, Kodansha, Tokyo, 1991, pp. 497–498.
[8] C.K. Costello, M.C. Kung, H.S. Oh, Y. Wang, H.H. Kung, Appl. Catal. A 232 (2002) 159.
[9] M. Haruta, T. Kobayashi, H. Sano, M. Yamada, Chem. Lett. 405 (1987).
[10] A. Manasilp, E. Gulari, Appl. Catal. B 37 (2002) 17.
[11] G. Gurdag, T. Hahn, Appl. Catal. A 192 (2000) 51.
[12] R.E.R. Colen, J. Christoph, F. Pena, H.H. Rotermund, Surf. Sci. 408 (1998) 310.
[13] V.V. Gorodetskii, A.V. Matveev, P.D. Cobden, B.E. Nieuwenhuys, J. Mol. Catal. A: Chem. 158 (2000) 155.
[14] G.Y. Wang, W.X. Zhang, H.L. Lian, D.Z. Jiang, T.H. Wu, Appl. Catal. A: Gen. 239 (2003) 1.
[15] B.D. Cullity, Elements of X-ray Diffraction, Addison–Wesley, Reading, MA, 1978.
[16] T.M. Salama, T. Shido, R. Ohnishi, M. Ichikawa, J. Phys. Chem. 100 (1996) 3688.
[17] J.R. Regalbuto, T.H. Fleisch, E.E. Wolf, J. Catal. 107 (1987) 114.
[18] G. Zhang, PhD Thesis, Stanford University, UM 8608245, 1985.
[19] T.M. Salama, T. Shido, H. Minagawa, M. Ichikawa, J. Catal. 152 (1995) 322.
[20] T.M. Salama, Z.M. El-Bahy, F. Zidan, under publication.
[21] A. Manasilp, E. Gulari, Appl. Catal. B 37 (2002) 17.
[22] O. Korotkikh, R. Farrauto, Catal. Today 62 (2000) 249.
[23] M. Haruta, T. Tsubota, T. Kobayashi, A. Ueda, H. Sakurai, M. Andom, Catal. Catal. (Shojvabal) 33 (1991) 440.
[24] M. Haruta, N. Yamad, T. Kobayashi, S. Iijima, J. Catal. 115 (1989) 301.
[25] T.M. Salama, Y. Ohnishi, M. Ichikawa, J. Chem. Soc., Faraday Trans. 92 (1996) 301.
[26] G.E. Glass, J.H. Konnert, M.G. Miles, D. Britton, R.S. Tobias, J. Am. Chem. Soc. 90 (1968) 1131.
[27] Y. Yuan, K. Akasura, H. Wan, K. Tsai, Y. Iwasawa, Catal. Lett. 42 (1996) 15.
[28] T.V. Choudhary, C. Sivadinarayana, C.C. Chusuei, A.K. Datye, J.P. Fackler Jr., D.W. Goodman, J. Catal. 207 (2002) 247.